PIV FLOW FIELD MEASUREMENTS OF ELECTROHYDRODYNAMIC CONDUCTION PUMPING

Michal Talmor [a], Christophe Louste [b], Jamal Seyed-Yagoobi [a]

[a] Multi-Scale Heat Transfer Lab
Dept. of Mechanical Engineering
Worcester Polytechnic Institute, Worcester MA
e-mail: mtalmor@wpi.edu, jyagoobi@wpi.edu

[b] PPRIME Institute
Dept. of Fluid Flow, Heat Transfer and Combustion
CNRS-University of Poitiers-ESMA, France
e-mail: christophe.louste@univ-poitiers.fr

***Abstract* - Electrohydrodynamic (EHD) conduction pumping utilizes the interaction between strong applied electric fields and naturally occurring electrolyte impurities within dielectric liquids. Comprised of series of electrode pairs and placed in contact with a dielectric liquid, EHD conduction pumps can be used to generate internal and external net flows, create circulation and mixing, distribute flow in parallel channels, and pump thin liquid films and two-phase flows. Most experiments performed using EHD conduction pumps have focused on global flow rate and pressure generation measurements, but have not provided measurements of the actual flow velocity fields generated by these pumps. While these flow velocity fields can be simulated numerically, both qualitative flow visualization and quantitative measurements of the true flow velocity vectors are difficult to accomplish for EHD conduction due to the presence of the strong electric field. Few studies have therefore attempted to perform any kind of flow visualization of EHD conduction pumping in general, and fewer still offered velocity measurements for these devices. This paper provides a comprehensive set of measurements of the flow velocity fields generated by a multi-electrode EHD conduction pump, measured using particle imaging velocimetry, with unique insulating particles as the visualization elements. These measurements were taken for several flow conditions that provide insight into the effect of external flow inertia on the EHD conduction pumping mechanism - static pressure generation with no net flow through the loop, open flow through the loop, and in the presence of externally applied flows supplied by a mechanical pump.**

I. INTRODUCTION

Electrohydrodynamic (EHD) pumping utilizes the interaction between Coulomb body forces, generated by electric fields applied on fluids, and charges within fluids in order to generate and control fluid flow. This state-of-the-art technology achieves significant flow motion without mechanical means or moving parts, and can be easily miniaturized. These properties make EHD pumping advantageous for applications such as electronics cooling and heat transfer enhancement [1]. Three types of EHD pumping mechanisms have been investigated, known as ion drag pumping, induction pumping, and conduction pumping.

These mechanisms differ from each other by the method each uses to introduce charges into the working fluid.

Ion drag pumping, or injection pumping, uses a corona discharge from a sharp emitter electrode in order to inject charges into the fluid [2].

Induction pumping depends on the existence of a gradient in the electrical conductivity of the fluid, due to an interface between different fluids or phases, or the presence of temperature gradients. Naturally occurring charges within the fluid accumulate in the locations of such property gradients and can be moved via a travelling AC electrical field due to the difference between the charge transit time and the charge relaxation time [3].

Conduction pumping, the mechanism studied in this work, utilizes strong electrical fields in order to enhance the dissociation reaction of naturally occurring electrolytic impurities within dielectric liquids. In equilibrium conditions, in the absence of a strong electric field, these naturally occurring impurities dissociate and recombine at equal rates, as shown in the following equation [4],

$$AB \underset{Recombination}{\overset{Dissociation}{\rightleftharpoons}} A^+ + B^- \tag{1}$$

Applying a strong electric field between two electrodes in contact with the working fluid increases the dissociation rate exponentially, while the rate of recombination remains relatively constant. The positive and negative charges formed in this manner are then attracted to the oppositely charged electrodes and migrate to them due to the electric field. A new equilibrium is then formed, in which the ions retain their charge as they travel within thin layers near each oppositely charged electrode, known as the heterocharge layers, while recombining and losing their charge outside of these layers [5].

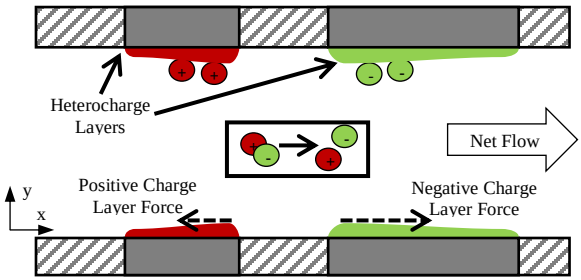

Fig. 1: EHD Conduction Pumping Mechanism

The greater the size of these space charge layers, and the greater the concentration of charge within them, the greater the Coulomb forces applied on the fluid. Since, for a given electrode pair, the two layers generate opposing forces on the fluid, if the wetted surface areas of the high voltage and ground electrodes are the same only mixing will occur. Therefore, EHD conduction pumps are designed with asymmetric electrodes, such that a net force is applied on the fluid, which creates a net flow in a desired direction. The EHD conduction pumping mechanism is illustrated in Figure 1, where the electrodes are flush with the wall.

Flow visualization of fluids under the effect of EHD forces has been previously performed primarily for ion drag pumping of gases, also known as the corona ionic wind. Most of the techniques used for such flow visualization have focused on exciting inserted fluorescent molecules via lasers [6]-[7], the Schlieren photography method for visualization of density changes [8], or gas phase Particle Imaging Velocimetry (PIV) [9]-[10].

Additional researchers have performed flow visualization experiments on ion drag pumping in the liquid phase using the Schlieren method for fluids, which relies on local changes in light refraction rather than density changes [11], as well as other techniques such as Laser Doppler Velocimetry (LDV) [12], Laser Doppler Anemometrya (LDA) [13], and liquid phase PIV [14]-[15]. LDA was also used for velocity measurements of EHD induction pumping of a stratified fluid film [16]. Other than the PIV and LDV/LDA methods, the other flow visualization techniques yielded only qualitative flow pattern images, rather than precise measurements of the flow velocities. In addition, the LDV/LDA method is only capable of providing measurements of velocities at discreet pre-determined points (probe volumes), rather than obtaining the full velocity field all at once.

Studies of two-phase flow visualization in the presence of an electric field have also been performed for liquid flows driven by interfacial forces exerted by ion drag pumping in a stratified medium, using the PIV technique [17], or micro PIV technique [18] for thin fluid films. Flow visualization of EHD conduction pumping either in single or two-phase flows, however, has not been well studied. The first study appearing in the literature is by Hemayatkhah et al. [19], who used dye infusion to generate a qualitative flow pattern map, as shown in Figure 2.

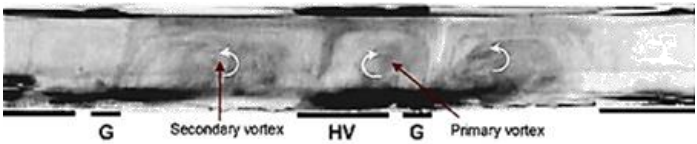

Fig. 2: EHD Conduction Pumping Dye Visualization [19]

In this figure, the EHD conduction pump electrode widths are 4mm and 12mm for the ground and high voltage electrodes, respectively, with a 2mm gap between said electrodes. The image shows a sub-section of the pump, which contained six electrode pairs. This study showed the characteristic vortices associated with EHD conduction pumping using flush electrodes, which had been previously only observed in numerical studies [20], such as in Figure 3. This figure shows the velocity streamlines generated by EHD conduction in a nondimensional simulation.

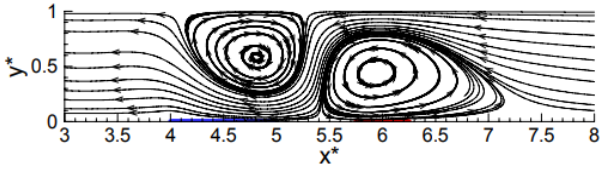

Fig. 3: Simulated EHD Conduction Velocity Streamlines [19]

Some initial studies using PIV flow field measurements have also been performed by Daaboul et al. [21] on a confined EHD conduction pump inside a rectangular test chamber,

and by Chirkov et al. [22] on an enclosure containing a barrier restriction. In both cases, only a single pair of electrodes was used, and the flow was circulating inside of an enclosure, without any net generated flow or flow loop.

To the authors' knowledge, no further work has been performed on EHD conduction pumping flow visualization. The purpose of this study is to provide a more comprehensive set of PIV based velocity field measurements for a multi-electrode EHD conduction pump driving a thin fluid film inside a flow loop, in the presence and absence of externally applied flows.

II. Particle Imaging Velocimetry

This measurement technique uses a laser sheet that briefly illuminates a vertical slice of a fluid containing small reflective seed particles, as shown in Figure 4. The light reflecting from the particles is captured by a camera positioned orthogonally to the laser sheet. Specialized PIV software can analyze two sequential captured images and identify particles that appear in both. The displacement of such particles and the time interval between the two images are then used to construct local velocity vectors.

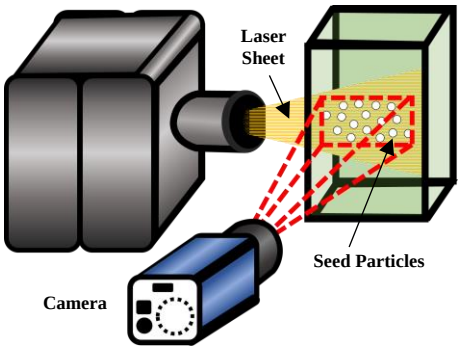

Fig. 4: PIV Measurement Schematic

The reflective seeding particles must be selected such that they provide an accurate representation of the flow they are carried by. In applications without a strong electric field merely controlling for the size of the particles is sufficient for quality measurements. However, due to the presence of the strong electric field in this work, it was essential that any charging of the seeding particles would be avoided. If these particles were charged, their movement and velocity would be due to migration along the electric field lines, rather than being representative of the actual fluid flow field [24]. In addition, if the seeding particles became attracted to the EHD conduction pump's electrodes and obscured their surface, it would have affected the pump's ability to generate the flow or caused a spark.

In order to ensure that the particles do not obtain a charge, they must be made of an insulating material, and the electric field must be turned off between measurement periods. With the field shut off, the particles must be allowed to circulate in the flow loop via a mechanical pump, in order to relax any small accumulations of charge that the particles may have gained during the measurement period.

In this work, the PIV measurements were taken using a LaVision acquisition system comprised of a category 4 double pulsed Nd: YAG laser and a high speed CCD digital camera with a spatial resolution of 1376×1040 pixels. The velocity fields were computed via the Lavision Davis 8.0 software package, using cross-correlation with a 50% overlap for an interrogation window of 16×16 pixels. Measurements were taken only for steady state flows, defined as allowing 90 seconds for the EHD conduction pump's current to reach a steady value. These measurements were then time averaged over a set of 1000 captures. The seeding particles used were from a PTFE Teflon powder with an average particle diameter of 200µm.

III. Experimental Setup

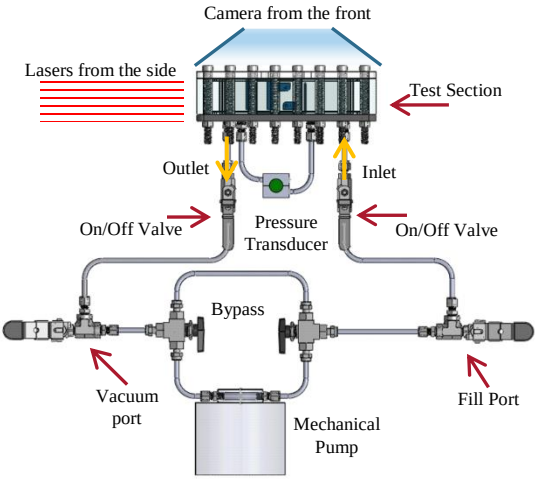

Fig. 5: Experimental Setup Schematic

A schematic of the experimental loop used in this work is shown in Figure 5. The 25cm x 13cm x 5cm test section housed the EHD conduction pump, and had highly polished, clear acrylic on three sides and a matt black polypropylene back on the fourth side. The laser sheet was projected into the test vessel through one of the clear acrylic 5cm wide sides, while external shielding placed against the opposite side prevents undue laser refraction. The high speed camera was facing the clear acrylic 25cm x 13cm side, and used the black side as a backdrop so that the particles could be captured clearly. Two valves were used to seal the test section from the rest of the loop. An ISMATEC BVP-Z model gear pump with a suction-shoe type pumping head able to deliver 102mL/min at 6000rpm was used to both apply an external flow on the EHD conduction pump, and to recirculate the particles to prevent sedimentation.

The EHD conduction pump assembly design is shown in Figure 6. The pump is comprised of three electrode pairs, designed as interlocking combs, with the electrode widths and spacing given in Table 1.

Table 1: EHD Conduction Pump Dimensions

Ground Electrode Width	3mm
Space Between Electrodes	3mm
High Voltage Electrode	9mm
Space Between Pairs	15mm

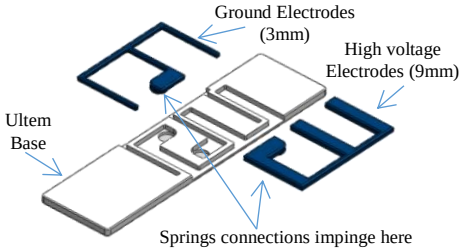

Fig. 6: Electrode Configuration Schematic

The electrodes were press-fit into an Ultem substrate, which served as electrical insulation between the electrodes, structural support for the assembly, and location setting for the electrodes. The tab shown in Figure 6 on each set of electrodes was connected to the high voltage and ground feedthrough inputs via springs loaded connectors, to ensure a secure contact. These feedthrough connections were inserted from the bottom of the housing. To ensure the tabs did not significantly affect the generated electrical field, and to maintain the minimum distance between all grounded parts and all parts connected to high voltage, the space between the first and second electrode pairs was increased to 25mm.

Fig. 7: Test Section with EHD Conduction Pump

Figure 7 shows the final assembly, where the pump is inserted into a track in the housing and pressed in on both sides by the front and back plates.

Power was supplied to the electrodes via a Spellman SL10 power supply with a maximum voltage and current ratings of 30kV 0.33mA.

TABLE 2: HFE-7000 PROPERTIES [25]

Dielectric Constant	7.4
Breakdown Voltage	15 kV/mm
Liquid Density	1400 kg/m^3
Kinematic Viscosity	0.32 cSt

The working fluid used in this study was the 3M HFE-7000 engineering fluid. This fluid's properties are shown in Table 2. The film height chosen for this experiment was 12mm, which represents a high enough height for PIV measurements to provide enough resolution of the velocity profile, but a low enough height for the flow to still be considered a thin film flow. The EHD conduction pump was tested both in the "static" case, where the valves isolated it from the rest of the loop, and the "dynamic" case where flow was allowed to circulate through the loop. In addition, the mechanical pump was used in order to oppose the EHD conduction pump, by applying an opposing flow rate of 15mL/min, which translates to an opposing flow velocity of 0.5 m/s.

IV. Results and Discussion

Figure 8 shows the behavior of the thin liquid film as captured by the high speed camera, at the maximum applied voltage of 20kV for all three cases studied – (a) the static case where the test section was isolated from the loop using the inlet and outlet valves, (b) the dynamic case where the valves were open and flow was allowed to circulate in the test loop while bypassing the mechanical pump, and (c) the opposed flow case where the mechanical pump was also connected to the loop and was actively opposing the EHD conduction pump's flow. In these images, the inlet and outlet are the fittings on the far left and far right of the image, respectively. The EHD conduction pump is positioned between $x = -45mm$ and $x = 40mm$, with the second electrode pair positioned between $x = -5mm$ and $x = 10mm$ and the third starting at $x = 25mm$.

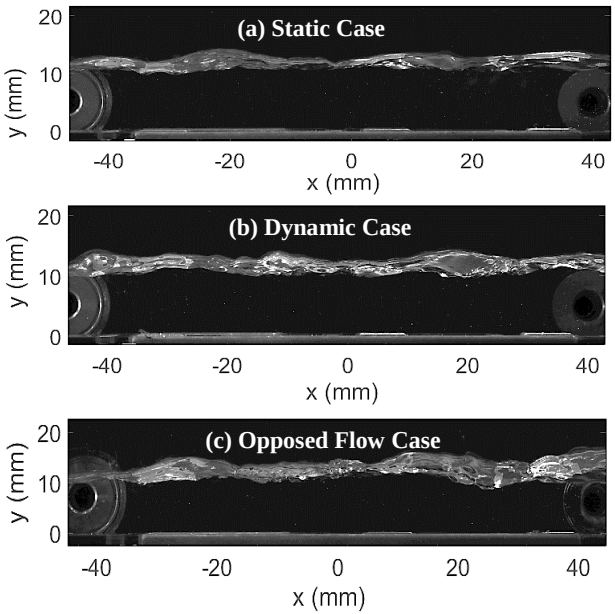

Fig. 8: All Cases at 20kV, Flow Waves

These images provide a qualitative view of a few of the characteristic differences between these cases that will be shown quantitatively in the velocity field measurement plots further on in this section. The static case presented in Figure 8a shows a waveform almost like a standing wave, since the flow is confined to the test section. The flow is also calmer than in the subsequent cases, such as the dynamic case presented in Figure 8b. In this case, the waves appear to be more irregular and there a subtle increase in the overall wave amplitude in the direction of flow. This is also seen in Figure 8c, which shows a significantly more choppy set of waves and the increase in amplitude in the positive x direction is more apparent. These qualitative trends are shown more qualitatively in Figures 9-12 which present the full flow field measurements taken at different applied voltages for each of the three cases.

Beginning with Figure 9, where 2kV is applied, a few general trends can be discerned. First, the formation of vortices within the film. These vortices originate from each electrode pair, with a clockwise vortex forming over the ground electrode and a counter-clockwise one forming over the high voltage electrodes. The two vortices then touch at the space between the electrodes, where the flow is pointing downwards. As shown, the velocity of the flow increases sharply after the trailing edge of the high voltage electrode, with an upward direction. This is the cause of the waviness shown in Figure 8.

Another trend of note is the maximum local flow velocities achieved in each case. While it is expected that in the static case, the pump would generate the most pressure, the overall flow is confined, so the resulting flow velocities are lower than in the dynamic case for all voltage levels higher than 8kV. In addition, the opposed flow case the velocities are higher than in all the other cases. This is due to the effect of the incoming velocity on the formation of the heterocharge layers over the electrodes. The opposing flow serves to lift the layers over the high voltage electrodes, such that they impinge more into the bulk of the fluid.

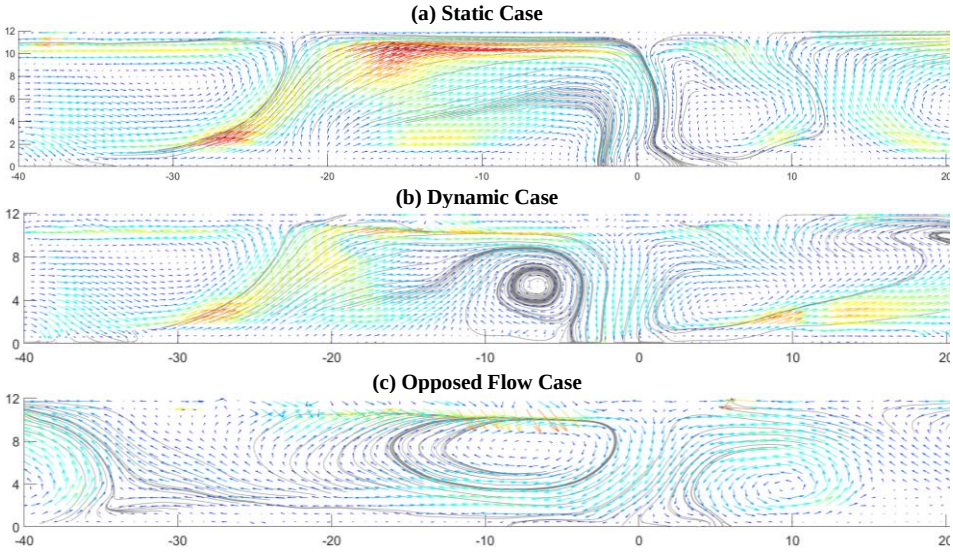

Fig. 9: Flow Fields, EHD Conduction Pump at 2kV

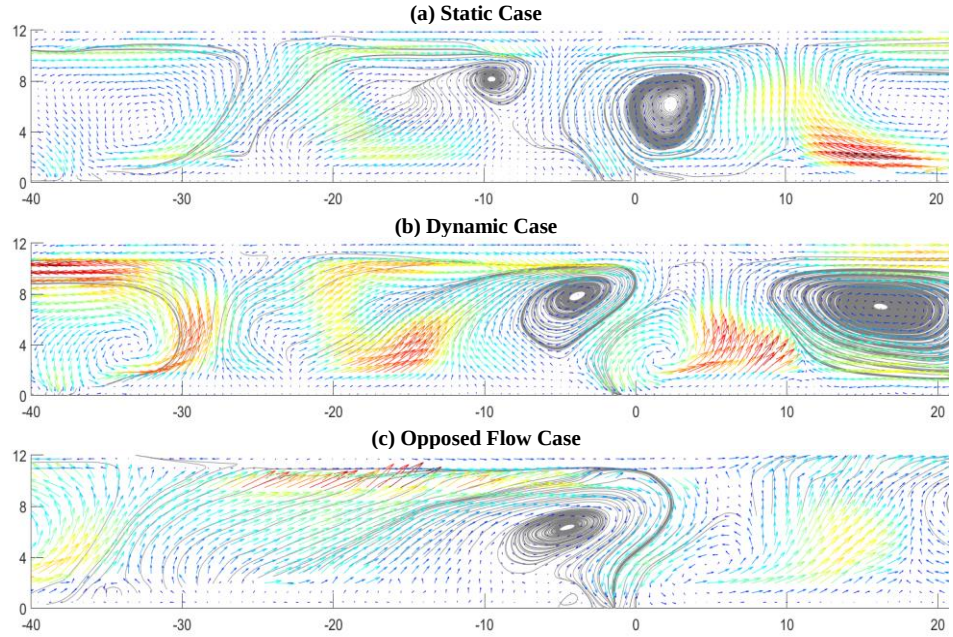

Fig. 10: Flow Fields, EHD Conduction Pump at 8kV

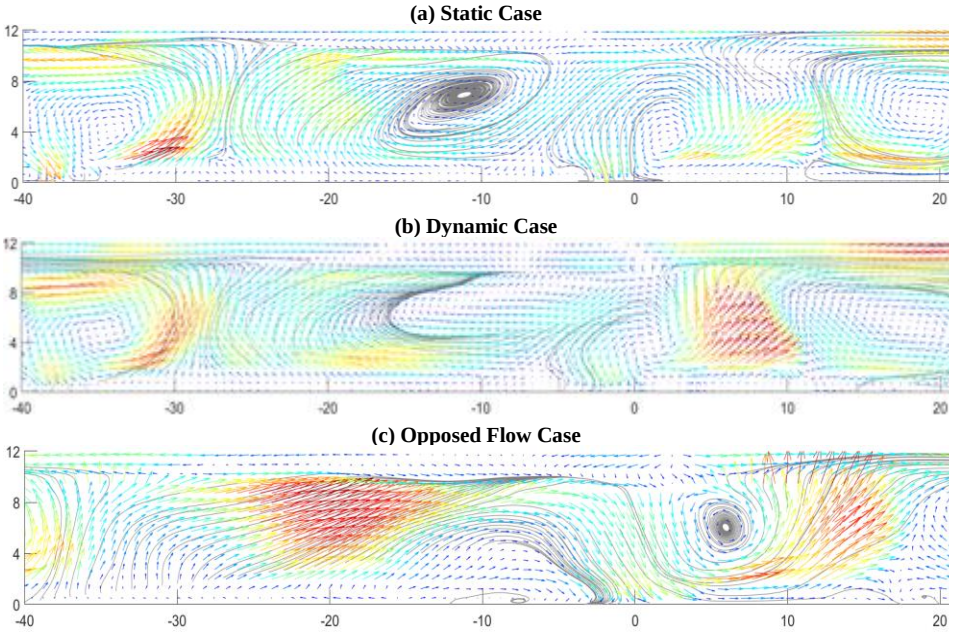

Fig. 10: Flow Fields, EHD Conduction Pump at 16kV

This increases the Coulomb forces generated from those charge layers, and increases the performance of the pump. This trend becomes increasingly pronounced with increasing voltage, to the point where the highest local velocity at 20kV is almost double that of the dynamic case.

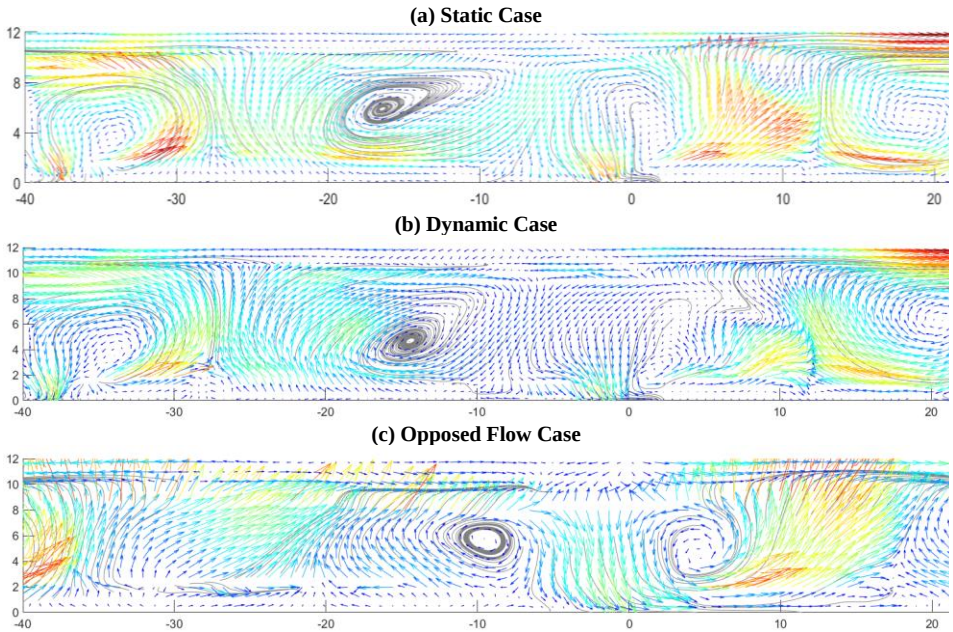

Fig. 11: Flow Fields, EHD Conduction Pump at 20kV

These observed trends are summarized in the graphs in Figures 13-15, which show the magnitudes of the maximum positive (in the positive x direction) and maximum negative (in the negative x direction) velocities on the surface of the film and in its bulk or core for each of the three cases for all applied voltages. Surface velocities are defined as the velocities within the top 1mm of the fluid film, whereas core velocities are anywhere below that.

In Figure 13a, the maximum positive film velocity and the maximum positive core velocity are mostly the same for all voltage levels. In addition, comparing the positive and negative velocities to each other provides a measure of the amount of circulation occurring in the test section. In Figure 13b, the core velocities show a tendency toward a flow in the negative direction for the range of voltages between 2kV and 14kV, meaning that the magnitude of the maximum negative velocity is greater than that of the positive one. However, this trend is not seen in Figure 14b, which shows the core velocities for the dynamic case. This implies that in the static case the circulation in the core is asymmetrical, where the flow might be bouncing off of the right hand side wall and the EHD conduction forces are not sufficient to maintain equal circulation in the core, unlike at higher voltages.

In addition, the positive and negative maximum surface velocities in Figure 13c are equivalent to each other, while they differ significantly in Figure 14c, and the mean surface velocity in Figure 13a is significantly lower than in Figure 14a. These differences are again

due to the flow confinement, since the flow does not have an easy path forward and out of the test section.

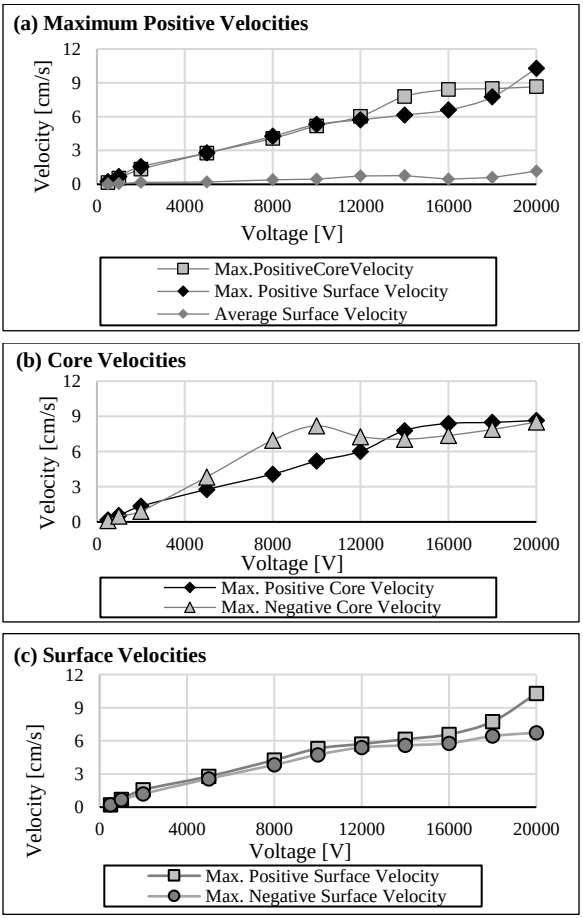

Figure 12: Static Case Maximum Velocities

Figure 14a shows how the situation differs when the flow is allowed to circulate through the loop. Here, both the core and surface velocities are higher than in Figure 13a, but the surface velocities outstrip the core. While the core is closer to the electrodes, where the primary flow driving forces are strongest, the core is also closer to the stationary wall, and has more fluid mass to contend with than the surface. Therefore, the fully developed and highest flow velocities are expected to be at the surface in this case. Figures 14b and 14c show that there is much more circulation in the core of the fluid than at its surface, since the negative and positive velocities in the core are equivalent to each other. This again shows that without confinement, the overall flow will move in the positive direction.

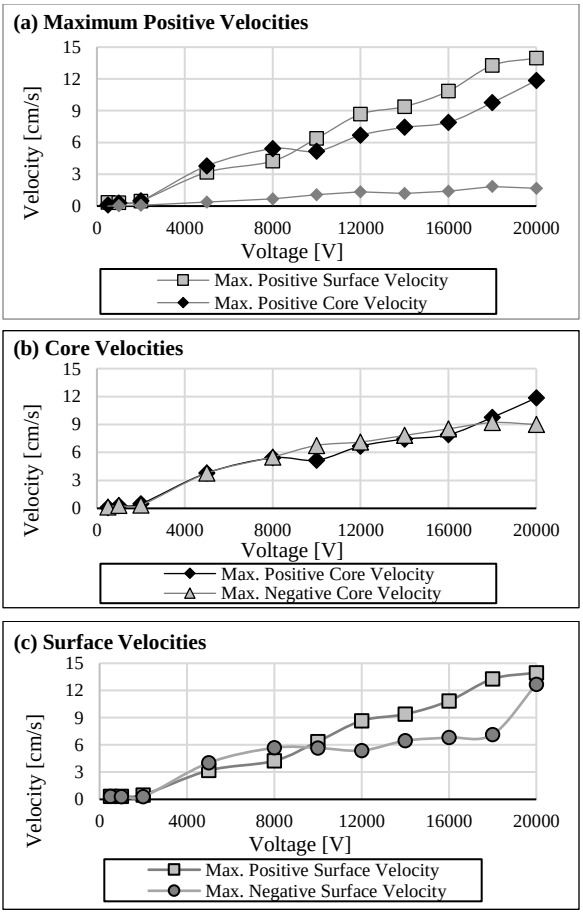

Figure 13: Dynamic Case Maximum Velocities

Lastly, Figure 15 shows the maximum core and surface velocity magnitudes for the opposing flow case. Here, the flow velocities are much higher than for the other cases. In Figure 15a, the surface and core velocities do not show a clear trend, and in Figure 15c the surface velocities are highly circulatory, only showing a net positive flow for the highest applied voltages. This is due to the opposing flow behaving as a sort of wall that the EHD conduction pump's flow must impinge on to obtain a net positive flow. In this case, we see a significant difference between the maximum positive and negative core velocities for higher voltages, since the EHD conduction forces in the positive direction are bolstered by the opposing flows. Therefore, in the opposing flow case the flow can be said to be core-driven, while in the dynamic case it is more surface-driven.

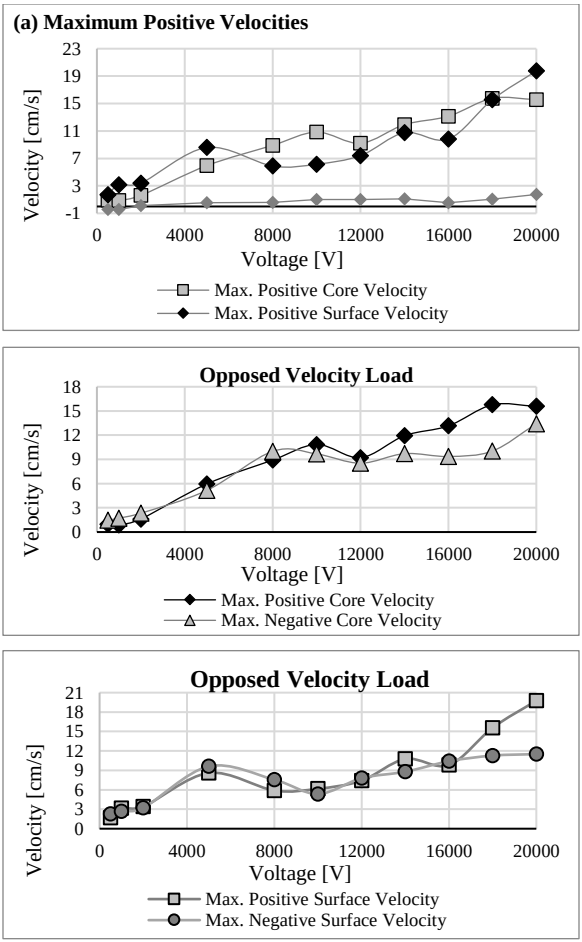

Fig. 14: Opposed Flow Case Maximum Velocities

V. Conclusion

The Particle Imaging Velocimetry (PIV) flow visualization and velocity field measurement technique was used on a multi-electrode EHD conduction pump pumping a 12mm film in different flow configurations. The results show that EHD conduction flows are highly circulatory, with vortices emerging in the vicinity of the electrodes, and subsequently generating waves on the film surface. In the core of the fluid, this circulation means that the net core velocity may be very small regardless of confinement. However, when unconfined the generated surface velocities are predominantly positive. Lastly, when there exists an opposing flow to the EHD conduction pump's generated flow, the result is a direct enhancement of the generated flow velocities and overall net surface velocities, due to the underlying charge formation mechanisms.

ACKNOWLEDGEMENTS

The work of the first author was sponsored by a NASA Space Technology Research Fellowship (NSTRF). The authors would also like to thank the PIV laser technicians and the manufacturing center at the PPrime Institute, at the CNRS University of Poitiers, France, for their assistance and support.

REFERENCES

[1] Seyed-Yagoobi, J., "Electrohydrodynamic pumping of dielectric liquids", *Journal of Electrostatics*, vol. 63, pp.861-869 (2005).

[2] Richter, A. and Sandmaier, H., "An electrohydrodynamic micropump", *In Proceedings of the IEEE Micro Electro Mechanical Systems*, pp. 99-104 (1990).

[3] Melcher, J. R., "Traveling-Wave Induced Electro-convection", *The Physics of Fluids*, vol. 9(8), pp. 1548-1555 (1966).

[4] Atten, P. and Seyed-Yagoobi, J., "Electrohydrodynamically induced dielectric liquid flow through pure conduction in point/plane geometry", *IEEE Transactions on Dielectrics and Electrical Insulation*, vol. 10(1), pp. 27-36 (2003).

[5] Pontiga, F. and Castellanos, A., "Electrical conduction of electrolyte solutions in nonpolar liquids", *IEEE Transactions on industry applications*, vol. 32(4), pp.816-824 (1996).

[6] Ohyama, R., Aoyagi, K., Kitahara, Y. and Ohkubo, Y., "Visualization of the local ionic wind profile in a DC corona discharge field by laser-induced phosphorescence emission", *Journal of visualization*, vol. 10(1), pp. 75-82 (2007).

[7] Kitahara, Y., Aoyagi, K. and Ohyama, R., "An experimental analysis of ionic wind velocity characteristics in a needle-plate electrode system by means of laser-induced phosphorescence", *Proceedings of the Annual Conference on Electrical Insulation and Dielectric Phenomena*, pp. 529-532 (2007).

[8] Sosa, R., Arnaud, E., Memin, E. and Artana, G., "Schlieren Image Velocimetry applied to EHD flows", *Proceedings of the International Symposium on Electrohydrodynamics*, pp. 331-334 (2006).

[9] Nakamura, H. and Ohyama, R., "An image analysis of positive ionic wind velocity under the DC corona discharge in needle-cylinder electrode system", Proceedings of the IEEE Conference on Electrical Insulation and Dielectric Phenomena, pp. 192-195 (2009).

[10] Kocik, M., Podlinski, J., Mizeraczyk, J. and Chang, J.S., "Particle image velocimetry measurements of wire-nonparallel plates type electrohydrodynamic gas pump", *IEEE Transactions on Dielectrics and Electrical Insulation*, vol. 16(2), pp. 312-319 (2009).

[11] Ohyama, R., Inoue, K. and Chang, J.S., "Schlieren optical visualization for transient EHD induced flow in a stratified dielectric liquid under gas-phase ac corona discharges", *Journal of Physics D: Applied Physics*, vol. 40(2), p.573 (2007).

[12] Daaboul, M., Louste, C. and Romat, H., "LDV measurements of liquid velocity induced by charge injection in Diesel oil in a blade-plane-slit geometry" *Journal of Physics: Conference Series*, vol. 142(1), p. 012041 (2008).

[13] McCluskey, F.M.J. and Perez, A.T., "The electrohydrodynamic plume between a line source of ions and a flat plate-theory and experiment", *IEEE Transactions on electrical insulation*, vol. 27(2), pp.334-341 (1992).

[14] Daaboul, M., Louste, C. and Romat, H., "Transient velocity induced by electric injection in blade-plane geometry", *Journal of Electrostatics*, vol. 67(2-3), pp.359-364 (2009).

[15] Yan, Z., Louste, C., Traoré, P. and Romat, H., "Velocity and turbulence intensity of an EHD impinging dielectric liquid jet in blade–plane geometry", *IEEE Transactions on Industry Applications*, vol. 49(5), pp.2314-2322 (2013).

[16] Wawzyniak, M., J. Seyed-Yagoobi, and G. L. Morrison. "An experimental study of electrohydrodynamic induction pumping of a stratified liquid/vapor medium." *Journal of heat transfer*, vol. 122(1), pp. 200-203 (2000).

[17] Ohyama, R., Kaneko, K. and Chang, J.S., "Flow visualization and image analysis of gas-phase AC corona discharge induced electrohydrodynamic liquid flow in a stratified fluid", *IEEE transactions on dielectrics and electrical insulation*, vol. 10(1), pp. 57-64 (2003).

[18] Qin, J.J., Yeo, L.Y. and Friend, J.R., "MicroPIV and micromixing study of corona wind induced microcentrifugation flows in a cylindrical cavity", *Journal of Microfluidics and Nanofluidics*, vol. 8(2), pp. 231-241 (2010).

[19] Hemayatkhah, M., Gharraei, R. and Esmaeilzadeh, E., "Flow pattern visualization of liquid film conduction pumping using flush mounted electrodes", *Experimental Thermal and Fluid Science*, vol. 35(6), pp.933-938 (2011).

[20] Yazdani, M. and Seyed-Yagoobi, J., "Electrically induced dielectric liquid film flow based on electric conduction phenomenon", *IEEE Transactions on dielectrics and electrical insulation*, vol. 16(3), pp. 768-777 (2009).

[21] Daaboul, M., Traoré, P., Vázquez, P. and Louste, C., "Study of the transition from conduction to injection in an electrohydrodynamic flow in blade-plane geometry", *Journal of Electrostatics*, vol. 88, pp.71-75 (2017).

[22] Chirkov, V.A., Komarov, D.K., Stishkov, Y.K. and Vasilkov, S.A., "Comparative analysis of numerical simulation and PIV experimental results for a flow caused by field-enhanced dissociation", *Journal of Physics: Conference Series*, vol. 646(1), p. 012033 (2015).

[23] Willert, C.E. and Gharib, M., "Digital particle image velocimetry", *Experiments in fluids*, vol. 10(4), pp.181-193 (1991).

[24] Daaboul, M., Louste, C. and Romat, H., "PIV measurements on charged plumes-influence of SiO 2 seeding particles on the electrical behavior" *IEEE Transactions on Dielectrics and Electrical Insulation*, vol. 16(2), pp.335-342 (2009).

[25] 3M, "3M™ Novec™ 7000 Engineered Fluid", 10316HB datasheet, issued November 2014.